Cell

Quantitative Proteomics Analysis of the Secretory Pathway

Annalyn Gilchrist,[1,6] Catherine E. Au,[1,6] Johan Hiding,[4,6] Alexander W. Bell,[1] Julia Fernandez-Rodriguez,[4] Souad Lesimple,[1] Hisao Nagaya,[1] Line Roy,[1] Sara J.C. Gosline,[2] Michael Hallett,[2] Jacques Paiement,[5] Robert E. Kearney,[3] Tommy Nilsson,[4,7] and John J.M. Bergeron[1,7,*]

[1] Department of Anatomy and Cell Biology, McGill University, 3640 University Street, Montreal, Quebec H3A 2B2, Canada

[2] McGill Centre for Bioinformatics, School of Computer Science

[3] Department of Biomedical Engineering

McGill University, 3775 University Street, Montreal, Quebec H3A 2B4, Canada

[4] Department of Medical and Clinical Genetics, Institute of Biomedicine and the Proteomics Centre at the Sahlgrenska Academy, Göteborg University, 413 90 Göteborg, Sweden

[5] Département de pathologie et biologie cellulaire, Université de Montréal, Montréal, Québec H3C 3J7, Canada

[6] These authors contributed equally to this work.

[7] These authors contributed equally to this work.

*Contact: john.bergeron@mcgill.ca

DOI 10.1016/j.cell.2006.10.036

SUMMARY

We report more than 1400 proteins of the secretory-pathway proteome and provide spatial information on the relative presence of each protein in the rough and smooth ER Golgi cisternae and Golgi-derived COPI vesicles. The data support a role for COPI vesicles in recycling and cisternal maturation, showing that Golgi-resident proteins are present at a higher concentration than secretory cargo. Of the 1400 proteins, 345 were identified as previously uncharacterized. Of these, 230 had their subcellular location deduced by proteomics. This study provides a comprehensive catalog of the ER and Golgi proteomes with insight into their identity and function.

INTRODUCTION

Proteomics has successfully mapped protein complements for several targets, including the nuclear pore complex in yeast (Rout et al., 2000) and clathrin-coated vesicles in rat brain and liver (Blondeau et al., 2004; Girard et al., 2005). There is evidence that these efforts have led to complete, accurate, and permanent catalogs: No additional proteins beyond those identified by Rout et al. (2000) have been identified as belonging to the nuclear pore complex, and the validity of each protein has been established. Beyond simple enumeration of the presence or absence of each individual protein in a sample, several studies (e.g., Blondeau et al., 2004; Foster et al., 2006; Kislinger et al., 2006) have also reported the relative abundance of each protein. One method gaining acceptance is to use the number of redundant peptides (obtained from tandem mass spectra) that identify a protein as a measure of the abundance of that protein. This opens up new avenues for the proteomics field. For example, the relative abundance of proteins can be clustered by similar expression profiles across tissues or organelles using standard clustering methods (Kislinger et al., 2006). Such techniques are used in microarray analysis and provide a convenient and visual way of understanding the overlap in protein composition and the associated distribution in relative abundance between compartments. This may point to common functions dictated by the compartment to which proteins cocluster.

A complete and accurate map of the secretory pathway remains elusive. For ER proteins, efforts such as HERA (Scott et al., 2004a) have compiled only 500 proteins related to folding chaperones, modifying enzymes, trafficking proteins, and signaling proteins through literature search and detailed curation. For Golgi proteins, the most comprehensive catalog contains 421 proteins characterized in Golgi fractions isolated from rat liver (Wu et al., 2004). However, the literature confirms the Golgi status of only 26% of these proteins.

This study represents a quantitative proteomic map of the rough ER, smooth ER, and Golgi apparatus isolated from rat liver homogenates. The use of highly enriched organelles and multiple biological replicates and the extension of the study to biochemical subfractions and organelle subcompartments as reported here provide experimental evidence indicating that COPI vesicles concentrate Golgi-resident proteins while largely excluding secretory cargo. In addition to uncovering 345 proteins of unknown function, these findings also open up new areas of investigation for the field.

RESULTS

Cell Map Strategy

A strategy was elaborated to map proteins to their intracellular locations using isolated subcellular organelles

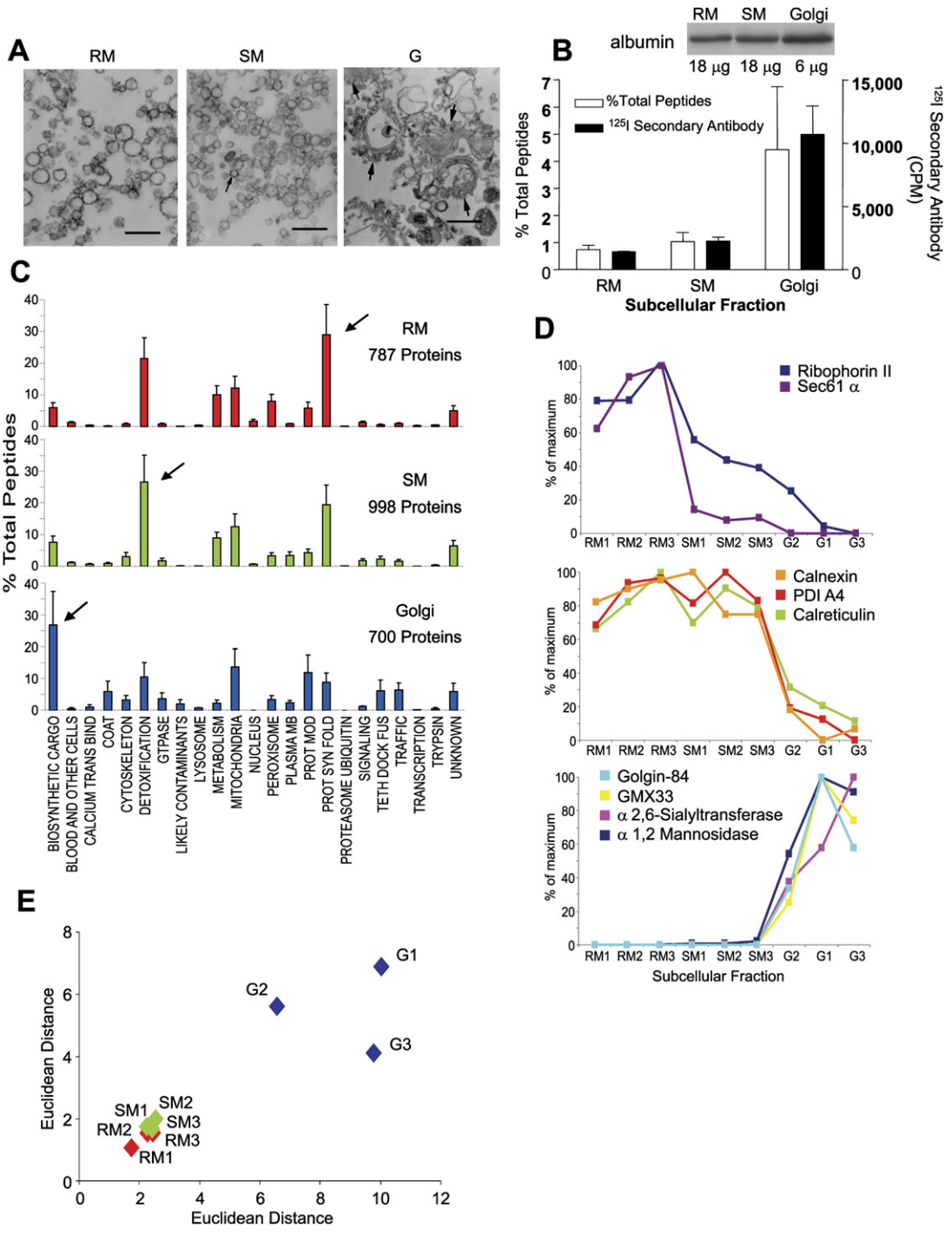

Figure 1. Proteomics of RM, SM, and Golgi Fractions Isolated from Rat Liver Homogenates

(A) EM characterization of random views of filtered preparations (Bell et al., 2001) of isolated rough microsomes (RM) with ribosome-studded microsomal profiles, smooth microsomes (SM) with a preponderance of smooth membranes but free polysomes (not shown) and occasional profiles showing ribosome-studded microsomes (arrow), and Golgi apparatus (G) with four different angles of section of Golgi profiles indicated by arrows. Scale bar = 0.5 µm.

(B) Comparison of redundant peptide counts with quantitative western blotting. The inset indicates the relative proportion of subcellular fractions within the linear response range for detecting albumin as visualized on X-ray films. The solid histograms represent the relative proportion of albumin antigenicity as deduced from γ counting (Bell et al., 2001) of the excised bands corresponding to albumin in RM, SM, and Golgi fractions. The white histograms represent peptide counts for albumin. In this and all other figures, error bars represent ±SD (n = 3) unless otherwise noted.

and tandem mass spectrometry. Isolated organelles were solubilized and their protein content was separated by SDS-PAGE. Each protein lane was cut into slices (~1 mm) and subjected to trypsin digestion followed by tandem mass spectrometry. To analyze derived data sets, we utilized a redundant peptide counting approach (Blondeau et al., 2004) as a quantitative representation of what the tandem mass spectrometer observed. The data are visualized as for microarray data (Cox et al., 2005; Kislinger et al., 2006). All tandem mass spectra were matched to the rat database with a confidence of >95%.

Organelle Isolation and Characterization

Well-established protocols were followed for isolation of RM (rough microsome), SM (smooth microsome), and Golgi fractions (Bell et al., 2001; Paiement et al., 2005). These subcellular fractions have been previously characterized by marker enzyme analysis, morphometry at the EM level to assess homogeneity, and a prior proteomics analysis for the Golgi fraction (Bell et al., 2001). Here, a random sampling methodology confirmed the homogeneity of these fractions (Figure 1A), although the SM fraction also contained contaminating free polyribosomes (data not shown). Enzyme analysis (see Figure S1A in the Supplemental Data available with this article online) confirmed the enrichment of the ER marker glucose-6-phosphatase in the RM and SM fractions and the Golgi marker galactosyltransferase in the Golgi fraction.

Quantitation of Tandem MS-Deduced Peptides

To test the validity of redundant peptide counting as an index of protein abundance in this study, we first compared this to quantitative western blotting using ^{125}I-labeled antibodies to albumin, the major secretory protein of liver (Figure 1B), which revealed a similar distribution. This distribution was also observed with independent experiments using the tandem mass spectrometer and the redundant peptide counting method. Indeed, comparison of redundant peptide counts with enzyme assays for glucose-6-phosphatase and galactosyltransferase confirmed that these marker enzymes were concentrated in the RM and SM or Golgi fractions, respectively (Figure S1A). A monotonic relationship between redundant peptide counts and protein abundance was also deduced from Figure S1B, in which increasing amounts of a SM fraction were applied to 1D SDS-PAGE. The results of the analysis of test protein samples are indicated in Figure S2, which further attests to the method as an index of protein abundance.

Analysis of RM, SM, and Golgi Fractions by Tandem MS: A Test for Homogeneity and Contamination

The results of the proteomics analysis (Tables S1A–S1D) are shown in Figure 1C (from Table S1D). All proteins and associated mass spectra were assigned to 23 categories, as described in the Supplemental Experimental Procedures. For RM, the highest number of peptides was for proteins involved in protein synthesis and folding; for SM, this category as well as proteins in the detoxification category showed the highest peptide abundance. Soluble biosynthetic cargo (largely plasma-destined proteins) was the most prominent on a peptide basis for Golgi fractions, as well as terminal sugar transferases and other protein modification enzymes of the protein modification category.

The redundant peptide counting method enabled a simple estimate of contamination by other organelles (Table S1D). As seen in Table S1D (for summary, see Table S2), peptides of mitochondrial proteins are by far the most prevalent, followed by peroxisomes. Western blot of plasma membrane markers suggested that plasma membrane proteins contaminated SM but not Golgi fractions (Figure S3). Regardless, all proteins annotated as plasma membrane were considered contaminants. Lysosomes and proteins derived from the nucleus were scarce (Table S1D) as deduced by redundant peptide counting (Table S2). The data in Table S2 estimate contaminants as ~20% of all assigned peptides. An independent estimate by morphometry of EM of the Golgi fractions suggested ~16% contamination, largely by endoplasmic reticulum (Bell et al., 2001). Mitochondria were only 1% of the volume of stacked Golgi cisternae. However, due to their dense proteinaceous content, ~10% of all peptides in Golgi fractions as deduced by proteomics are attributed to the mitochondria.

In order to assess the degree of crosscontamination among the isolated organelles, we selected a subset of proteins considered markers for the ER and Golgi apparatus. As illustrated in Figure 1D, redundant peptides assigned to the translocon constituent sec61α are highly enriched in the three biological isolates of RM fractions. Less sec61α peptides are observed in the three SM fractions, and only a few peptides are observed in the three Golgi fractions. The oligosaccharyltransferase constituent ribophorin II is also highly enriched in the three RM fractions, but with a significant proportion seen in the three SM fractions and a variable, low amount observed in the three Golgi fractions. Proteins expected to be equally distributed between the rough and smooth ER (e.g., calreticulin,

(C) Quantitative distribution of peptides assigned to proteins classified into 23 functional categories. A total of 35,645 tandem mass spectra were assigned to proteins in the indicated 23 categories. The arrows indicate the categories with the highest abundance of peptides for each subcellular fraction.

(D) Crosscontamination of ER (RM and SM) and Golgi fractions (G). Shown are peptide counts for each biological replicate (indicated as RM1, RM2, RM3, etc.) normalized to the highest concentration of the markers observed in any biological replicate. The maximal value (% total peptides) was set as 100%, and all other % total peptides were normalized to this 100%.

(E) Principal coordinate analysis (PCA) of the biological replicates (n = 1, 2, 3) of RM and SM fractions and their distinctiveness from the Golgi fractions. Data are from Table S1D.

the protein disulfide isomerase A4, and calnexin) indeed revealed such a distribution, with a variable, low amount detected in the three Golgi fractions. Golgi-resident proteins were largely enriched in the Golgi fractions, with few peptides detected for these proteins in the RM and SM fractions (Figure 1D). From these selected proteins, the ER character of the RM and SM fractions is evident, as is the Golgi character of the Golgi fractions.

We next applied hierarchical clustering commonly used for microarray analysis to the proteomics results of the RM, SM, and Golgi fractions. When these data were subjected to principal coordinate analysis (PCA) (Figure 1E), the areas encompassed by the RM and SM fractions overlap and are distinct from that of the Golgi. However, as predicted from the selected data represented in Figure 1D, the n = 2 Golgi fraction is more contaminated with ER and occupies a point in closer proximity to the ER fractions. Hence, PCA affirms that the variability among replicate isolations of a single organelle is much smaller than the differences between the organelles (ER and Golgi). Again, the use of hierarchical clustering with a Pearson correlation was used to visualize protein abundance measures (Figure S4). Since confounding organellar contaminants as well as other likely sources of contamination (keratins, trypsin, and proteins from cells of nonhepatic origin) were readily identified (Table S2), these 320 proteins were removed from the analysis (Figure 2A).

Closer analysis of selected clusters (Figure 2B) revealed proteins that cocluster with sec61, calnexin, p97, and mannosidase II (MannII). The most abundant proteins in the RM-associated sec61 cluster included the J domain and Brl domain-containing translocon constituent sec63 (Jermy et al., 2006). Other proteins in this cluster were the ribosome and nascent chain-associated NAC proteins (NACα and BTF3) as well as a ubiquitin-conjugating enzyme. Prominent proteins included the postulated RNA-binding protein vigilin (Goolsby and Shapiro, 2003) as well as several other RNA-binding proteins (see Table S4). Proteins that coclustered with calnexin included glucosidase II, protein-folding enzymes such as PDI and Ero1, which provides the reducing equivalents for the oxidizing environment of the ER, peptidyl *cis-trans* isomerase, and the hypoxia-upregulated stress protein GRP170. Moreover, abundant proteins characteristic of the liver ER were also found in this cluster. These included NADPH cytochrome P450 reductase, which is responsible for controlling electron flow through each of the more than 35 cytochrome P450s characterized in the ER proteome, and the metabolic enzyme transketolase of the pentose phosphate shunt, which is involved in glucose metabolism and is a target for cancer therapy (Langbein et al., 2006). A cluster with proteins mainly concentrated in smooth microsomes included the AAA family member p97 as well as the glycoprotein folding sensor UGGT and an abundant Ca/Mg ATPase related to that of the sarcoplasmic reticulum. Also found in this cluster was reticulon 3 protein, a constituent of a family of proteins implicated in the tubular structure of the smooth ER (Voeltz et al., 2006). This cluster also contained BAP31 and Gas2 proteins, which are causally implicated in apoptosis (Benetti et al., 2001; Stojanovic et al., 2005).

An unexpected finding was that the RDEL-terminating PDI family member ERp44 codistributed with ERGIC-53, four p24 family members, and MannII (Figure 2B). This was confirmed by indirect immunofluorescence using a polyclonal antibody to ERp44 that revealed a predominant juxtanuclear staining (Figure 2C) largely overlapping in staining with the Golgi marker GM130 (Figure 2C, merged). Some reticular ER-like staining was also found, consistent with the redundant peptide counts.

Biochemical Subfractionation of RM and SM Fractions to Extend the ER Proteome

The most abundant protein in the RM, SM, and Golgi fractions was serum albumin, with 570 redundant peptides in nine experiments. Hence, only two orders of magnitude were available for the detection of less abundant proteins. In order to detect these proteins, membranes were biochemically subfractionated by salt wash (S) to concentrate cytosolic membrane peripheral proteins followed by detergent extraction with Triton X-114 and phase separation to separate the soluble and lumenal proteins from the membrane proteins based on their partition into the aqueous (A) or the detergent (D) phase, respectively (Bordier, 1981). Figure S4B shows the hierarchical clustering of n = 3 replicates of the biochemical subfractions of RM and SM, and Figure 3A shows the hierarchical clustering of the mean values for each biochemical subfraction. Six clusters (Figure 3A) correspond to 77% of all of the assigned peptides (see Table S3B). Remarkably, these six clusters define proteins restricted to a limited number of functional categories, as represented with histograms in Figure 3B. Analysis of the individual proteins representing those in the most abundant categories (indicated by arrows in Figure 3B) is shown in Figure 3C. Notably, for the BiP cluster, most proteins were molecular chaperones and protein-folding enzymes known to be soluble luminal ER proteins and largely observed to be in the aqueous phase after Triton X-114 partitioning. The actin cluster constituted largely insoluble cytoskeletal proteins including molecular motors (kinesin family protein 13A, various myosins, and several components of the dynein/dynactin complex) and was largely localized to smooth microsomes.

Several proteins were insoluble in Triton X-114. Those insoluble proteins concentrated in RM and were largely ribonucleoproteins, RNA splicing factors, and DnaJ paralogs of as yet uncertain mechanistic significance that coclustered with the poly(A)-binding protein in the rough ER fraction. That these proteins were not removed by high salt suggests a strong interaction with the membrane of the rough ER. Similarly, the significance of the arginase cluster, consisting of metabolic enzymes removed by high salt and therefore loosely associated with the cytosolic surface of the rough ER, remains unknown. This cluster also contains elongation factor 2 and consists largely of

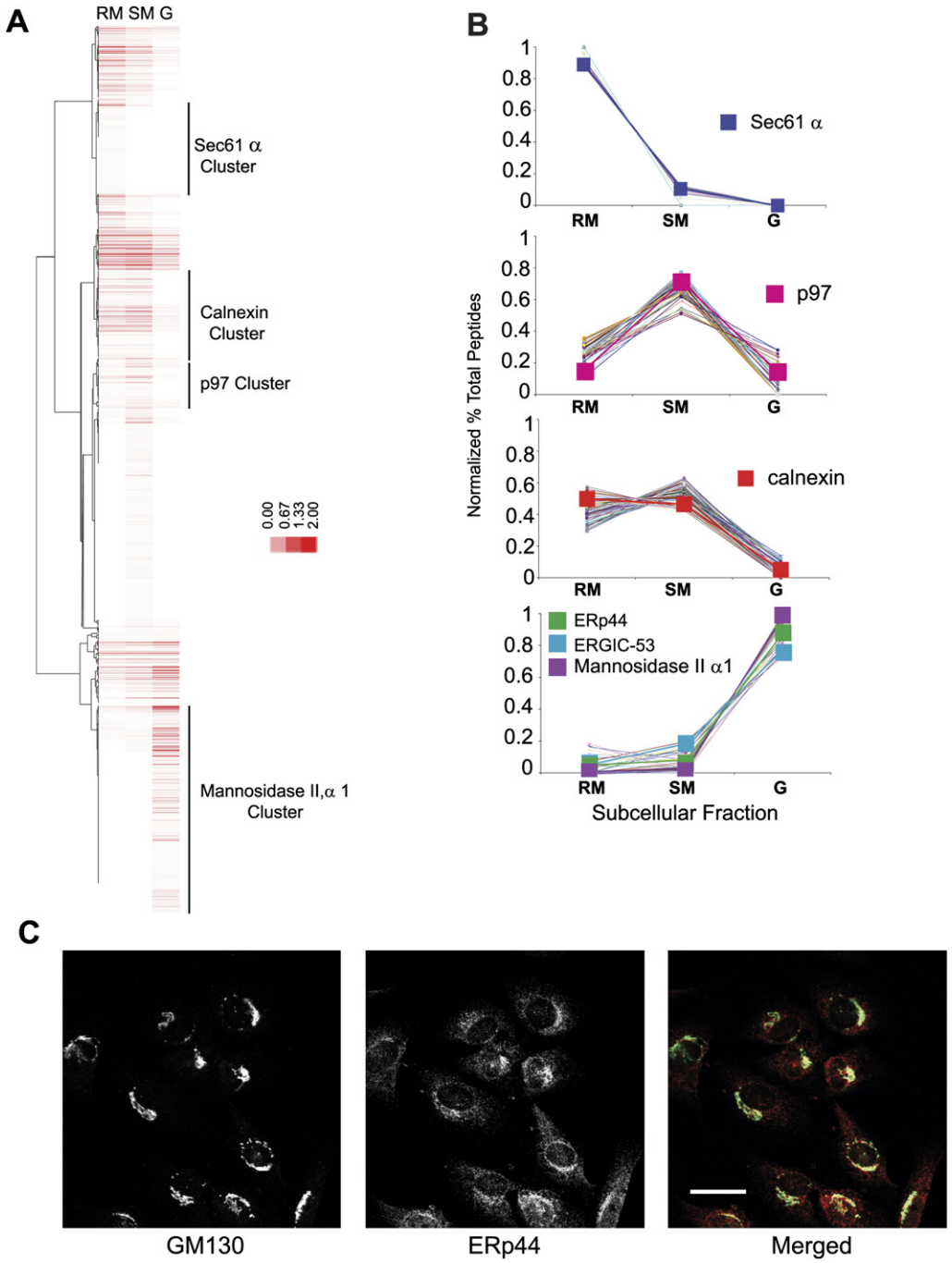

Figure 2. Hierarchical Clustering of Proteins that Codistribute with sec61, p97, Calnexin, and MannII and Immunolocalization of ERp44

(A) The RM, SM, and Golgi data (n = 3) from Table S1D (% total peptides) were averaged (Table S3) and used to generate the heat map. Clusters that contained sec61, p97, calnexin, and MannII as markers were selected (Pearson correlation coefficient > 0.90).

(B) Mean values for proteins in each of these clusters (Table S3) were plotted individually (Normalized % Total Peptides). ERp44, a RDEL-terminating member of the ER protein disulfide isomerase family, coclusters with the Golgi marker MannII (correlation coefficient > 0.95).

(C) Indirect immunofluorescence of ERp44 reveals a dual Golgi and ER localization as seen by colocalization with the *cis*-Golgi marker GM130. Scale bar = 25 μm.

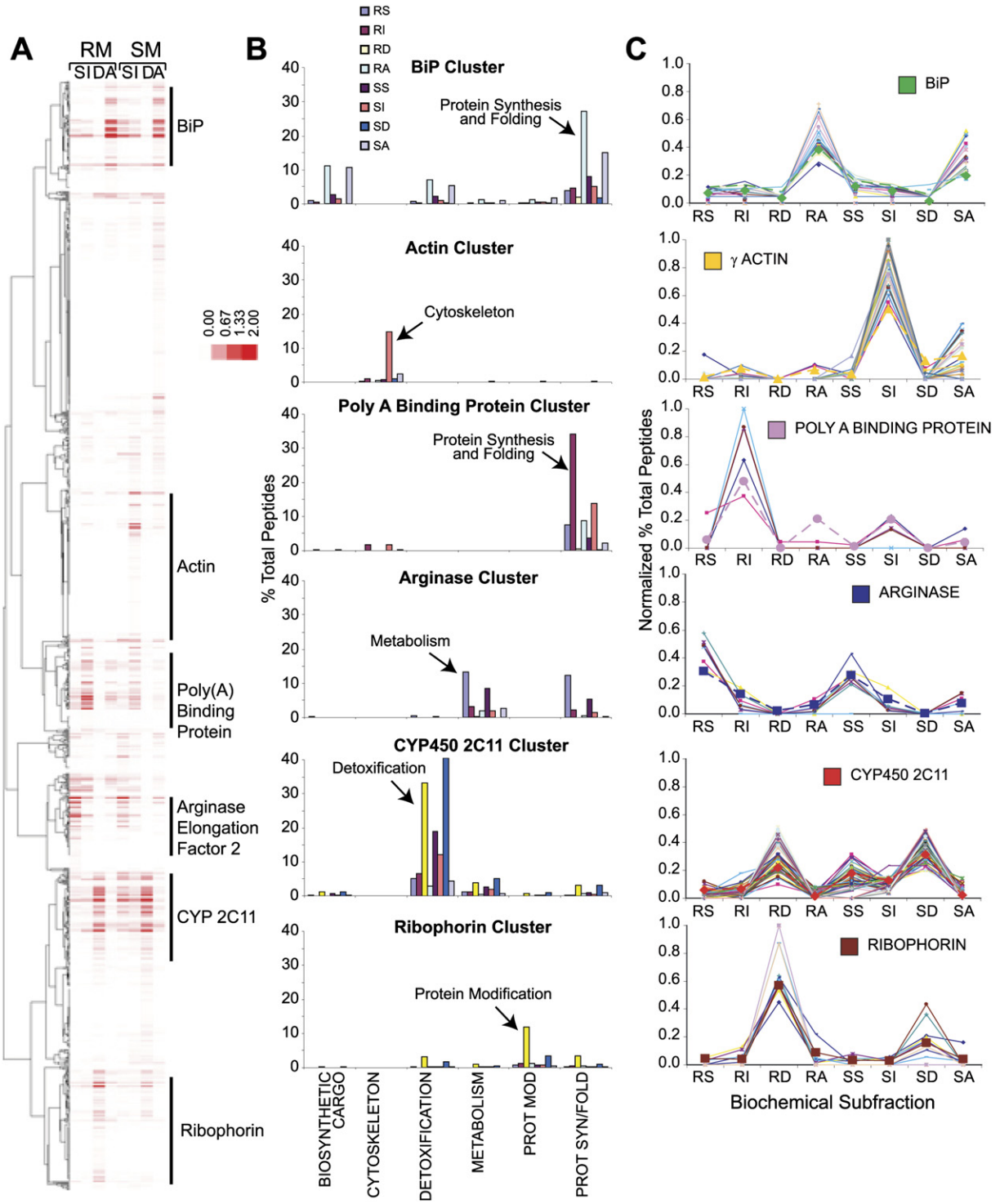

Figure 3. Protein Clusters in Biochemical Extracts from RM and SM Fractions

RM and SM fractions were extracted with high salt to give a salt wash fraction (S). This was followed by solubilization with Triton X-114 and resulted in a detergent-resistant insoluble fraction (I). The detergent-soluble proteins were further partitioned into detergent (D) and aqueous (A) fractions following a temperature shift as outlined in the Supplemental Experimental Procedures.

(A) Hierarchical clustering using Pearson correlation of the mean total % peptide counts of the three biological replicates for each biochemical fraction of the RM and SM was performed (Table S3B). Shown are the BiP cluster, the actin cluster, the poly A binding protein cluster, the arginase and elongation factor 2 cluster, the cytochrome P450 cluster, and the ribophorin cluster.

proteins involved in translation or folding. The cytochrome P450 cluster reflects a major function of the ER in lipid and steroid oxidation and drug detoxification. Finally, the ribophorin cluster defines integral membrane proteins (TX-114 soluble phase) of major functional significance in the endoplasmic reticulum for protein modification reactions that include N-linked glycosylation. Indeed, detailed analysis of all clusters (Table S3B) supports the conclusion that biochemical subfractionation of the RM and SM fractions led to the concentration of proteins with specific suborganellar locations. This extended the ER proteome by 35% (463 proteins, contaminants excluded, as deduced from Table S1D and Table S2).

Extension of the Golgi Proteome

Golgi membranes were treated in a fashion similar to the RM and SM fractions. As deduced from Table S4, this did not extend the Golgi proteome significantly. A total of 43 additional proteins were identified using this approach, yielding little insight over our previous work (Bell et al., 2001). Therefore, we incubated the Golgi membranes with cytosol to form COPI vesicles and isolated these through sedimentation and flotation for further analysis. The protocol used, which has been previously validated by us and reviewed by others (Rabouille and Klumperman, 2005), allows for the formation of vesicles that form in a COPI-specific manner. This requires the presence of cytosol, an ATP-regenerating system, and GTP hydrolysis. Very few vesicles are generated merely as a consequence of mechanical fragmentation (Kartberg et al., 2005; Lanoix et al., 1999; see also morphometry of Golgi fractions in Figure S5). The ARF-GAP required for ARF-1-specific sorting is supplied by the cytosol along with other factors. As vesicles can readily fuse once formed, the reaction mixture was supplemented with a recombinant and dominant mutant of α-SNAP to inhibit NSF-specific fusion. Figure 4 shows the homogeneity of the vesicles, with a diameter distribution largely of 45–60 nm (Figures 4A–4F). Larger structures were seen on occasion (Figure 4E) and were accounted for in the quantitation. A vesicle fraction where GTP hydrolysis was inhibited by addition of the nonhydrolyzable GTP analog GTPγS was also generated. These vesicles were found to have a broader diameter distribution (45–75 nm, Figures 4G–4L), possibly due to a higher degree of coated vesicles in the presence of GTPγS.

The results shown in Table S1D allow for an estimate for contamination of these vesicles (Figure 4M) to a maximum of 20% by ER. Contamination from other organelles is summarized in Table S2. PCA using the Euclidean metric (Figure 4N) reveals the distinctness of the COPI vesicle fractions (generated with hydrolyzable GTP) as compared to the COPI GTPγS vesicle fractions or Golgi fractions.

Quantitative representation of protein abundance (Figure S6A; Table S1D) enabled us to develop new concepts in the functions of Golgi and COPI vesicles. The Golgi fraction (G) indicates a prevalence of proteins representing soluble secretory cargo (plasma-destined proteins), while COPI vesicles (C) reveal a prevalence of proteins involved in posttranslational modification reactions (largely glycosylation enzymes). COPI GTPγS vesicles (γ) revealed coat proteins, although they also exhibit a broader distribution of proteins in the 23 functional categories. A total of 1191 different proteins were characterized, of which 279 were other organellar contaminants as identified in Table S1D and Table S2. After removal of the contaminants, hierarchical clustering (912 proteins; Figure S6B) was used to compare the protein expression data.

The experiments were highly reproducible (Table S1D; Figure S6B). Based on the reproducibility, the mean values for n = 3 experiments for each fraction were used; hierarchical clustering of these data is shown in Figure S7A. Figure S7B shows nine of the clusters in more detail, representing 71% of the peptides. The Rab6 and p115 clusters (which represent proteins restricted to Golgi cisternae) predominantly contain proteins that, with a very high degree of certainty, can be classified as biosynthetic cargo. These include serum albumin, of high abundance in the G fraction but present in a 2-fold-reduced amount in the C and γ fractions. Apolipoprotein B, another abundant cargo of the hepatic cell, is equally decreased in the two vesicle fractions, C and γ (Figure S7B, p115 cluster). These data are consistent with earlier immunogold-based labeling studies of thin frozen sections of both hepatic (Dahan et al., 1994) and pancreatic cells (Martinez-Menarguez et al., 2001), revealing a diminishment of soluble synthetic cargo in peri-Golgi vesicles including both albumin and apolipoprotein E (Dahan et al., 1994). Additionally, these clusters include Rab6 and Rab33b, two small GTPases involved in COPI-independent Golgi-to-ER recycling (Girod et al., 1999; Valsdottir et al., 2001). Syntaxin 5 (a Q-SNARE with a less polarized distribution across the Golgi stack; Hay et al., 1998), p97, and γ-SNAP were also found more frequently in the G fraction, as were the clathrin heavy chain and rSly1p. The latter is a SNARE-interacting protein belonging to the Sec1/Munc18 family of proteins, which are all central to the regulation of intracellular protein transport (for review, see Peng, 2005).

That the clathrin heavy chain (but not light chain) distributed to the p115 cluster (Table S3C) may be indicative of contamination with clathrin-coated vesicles. The removal

(B) The categories of proteins observed for each cluster, with the particular biochemical extract identified by color as seen in the boxes in the legend. Not all 23 categories are shown; the major categories are indicated by arrows. RS = RM salt wash, RI = RM insoluble, RD = RM detergent, RA = RM aqueous, SS = SM salt wash, SI = SM insoluble, SD = SM detergent, SA = SM aqueous.

(C) Distribution of proteins among the biochemical fractions that cocluster (Table S3B). The most prominent protein in each cluster (excluding the ribosomal proteins) is indicated by a dashed line.

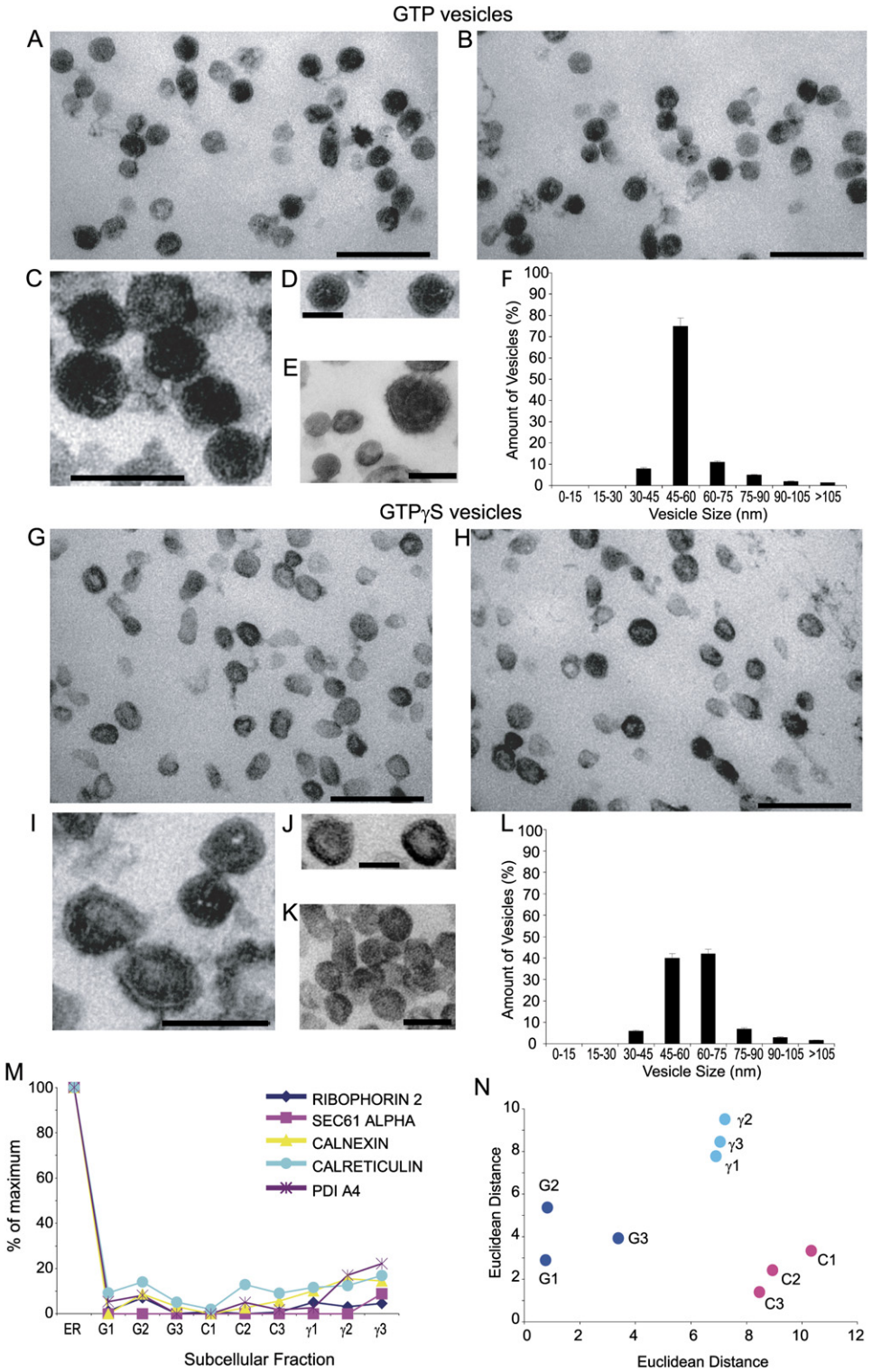

Figure 4. Morphology and Proteomics of COPI Vesicle Fractions

Ultrathin sections of floated vesicles reveal predominantly intact and homogenous vesicle populations. Vesicle fractions have been treated with tannic acid to reveal coat structures. Vesicles were generated by incubating purified rat liver Golgi with cytosol in the absence (A–F) or presence (G–L) of the nonhydrolyzable GTP analog GTPγS.

(A, B, G, and H) Random fields of vesicles from processed fractions. Scale bars = 250 nm.

of coatomer from the cytosol, however, results in a near complete diminishment of vesicular profiles observed in the vesicle fraction (Lanoix et al., 1999). The ARF exchange factor GBF1 was also largely depleted from the vesicle fractions, consistent with its function in promoting GDP-to-GTP exchange on ARF proteins on the cisternal membranes of the Golgi apparatus.

For the p24 cluster, two family members (β and γ) were nearly equal in the G, C, and γ fractions. Most of the COPI coat components (5 of the expected 7) were found in the COPI cluster. The two isoforms of γCOP, 1 and 2, were readily identified, indicating that more than one class of COPI vesicles was represented in the vesicle fraction (Wegmann et al., 2004). All coat components increased in abundance in the γ fraction as compared to the C fraction, indicating that the former contained more coated structures, consistent with the broader diameter distribution found in this fraction. Taken together, the COPI coatomer cluster highlights the COPI nature of the C and γ fractions. A related cluster, the ERV29 cluster, highlights proteins enriched only in the γ fraction. This cluster contains mostly ER proteins (dominated by ER detoxification enzymes), albeit at low amounts (see Table S1D). This would suggest that the γ fraction, even though clearly distinct (Table S1D), does not represent a faithful extension of the Golgi proteome in that non-Golgi ER contaminants accumulate therein. Therefore, we used the γ fraction only to explore the behavior of proteins that are also found in the G and C fractions (e.g., the COPI coat proteins).

The remaining clusters presented in Figure S7B highlight proteins that are enriched to a greater extent in the C fraction than in the G fraction and, to a different extent, the γ fraction. The Rab1 cluster contains Rab1 and Rab2 as well as the SNARE proteins rBET1 and Gos-28. MannII is also present in this cluster, which belongs to the larger family of glycosylation enzymes dominating but not exclusive to this cluster. The cluster with Vti-1b, a SNARE protein implicated in regulated secretion (Murray et al., 2005), also reveals a sec22 sequence homolog of unknown function, sec22A (Hay et al., 1996), as well as one of the key regulatory enzymes in gluconeogenesis (a major function of the liver), fructose 1,6-bisphosphatase (FBP). This cluster is also dominated by enzymes involved in protein modification (i.e., glycosylation enzymes) and the protein calnuc (Le-Niculescu et al., 2005). The membrin cluster contains proteins that are more equally distributed between the two vesicle fractions than the G fraction. The coatomer component β′ is found in this cluster, as are two SNARE proteins, sec22b and membrin. The Golgin 84 cluster also contains CASP. These were used previously to highlight different COPI vesicles (Malsam et al., 2005) formed in vitro. That both are enriched in the C fraction further highlights the COPI nature of this fraction. Furthermore, nine of the previously uncharacterized proteins in our extended Golgi proteome were found in this cluster. An attempt to define the cargo of COPI vesicles is illustrated in Figure 5. The analysis of nine abundant secretory cargo proteins in three different biological replicates of RM, SM, Golgi, and COPI vesicle fractions generated with either hydrolyzable (C) or nonhydrolyzable (γ) GTP revealed a reproducible enrichment and concentration of these proteins in Golgi cisternae (Figure 5A). An exclusion of these proteins in COPI vesicles was found that for several was near complete. This depletion was maximal for COPI vesicles generated with hydrolyzable GTP (C).

The opposite result was seen with resident Golgi proteins (Figure 5B). Here, maximal enrichment in concentration was observed in COPI vesicles, but only if these were generated with hydrolyzable GTP. For these Golgi-resident proteins, their concentrations in COPI vesicles (C) were in all cases higher than in Golgi cisternae. However, the enrichment of MannII was not as marked as GalNac-T1 in COPI vesicles, suggesting differences in degrees of sorting. In a strict cisternal maturation scheme, these results are unexpected, warranting further studies.

A Proteome of the Secretory Pathway

A schematic overview of the proteome of the secretory pathway is presented in Figure 6A depicting the number of proteins unique to the ER (832) and the Golgi (193) and proteins that occupy both the ER and the Golgi (405). After removing contaminants and biosynthetic cargo, we conclude that 832 proteins are constituents of the endoplasmic reticulum with no peptides detected in Golgi/COPI vesicles. These largely correspond to ribosomal proteins, translocon constituents, molecular chaperones, and proteins involved in lipid oxidation and drug detoxification, as well as proteasome subunits and ubiquitin ligases speculated to be involved in ERAD (Table S5A). For the 193 proteins found only in Golgi/COPI vesicles (no peptides detected in ER fractions), terminal sugar transferases, CASP, Golgin, SNAREs, and a subset of Rabs and COGs were prominent. The 405 proteins shared between the ER and the Golgi varied from those more enriched in Golgi (e.g., calnuc) to those more enriched in the ER (e.g., cytochrome P450s) as well as trafficking

(C, D, I, and J) Higher magnifications of discrete vesicles. Scale bars = 100 nm (C and I) and 50 nm (D and J).

(E and K) Large vesicles (E) and clusters of vesicles (K) are seen occasionally. Scale bars = 100 nm.

(F and L) Size distributions of vesicles in the two fractions. In the absence of GTPγS, vesicle profiles had an average diameter distribution of 45–60 nm (F), whereas in the presence of GTPγS, vesicle profiles had an average diameter distribution of 45–75 nm (L). The larger diameter distribution seen in (L) is consistent with a coat. Roughly 800 vesicle profiles were measured in each fraction. The difference in darkness between (A)–(E) and (G)–(K) reflects variation in the degree of tannic-acid staining.

(M) Selected known ER markers were assessed for peptide counts in the isolated subcellular fractions (ER, Golgi [G], COPI vesicles [C], and COPI GTPγS vesicles [γ]) and normalized to the highest concentration of the markers in the ER fraction. The biological replicate is indicated after the fraction (e.g., G1 = Golgi n = 1).

(N) Principal component analysis of Golgi, COPI vesicles, and COPI GTPγS vesicle fractions.

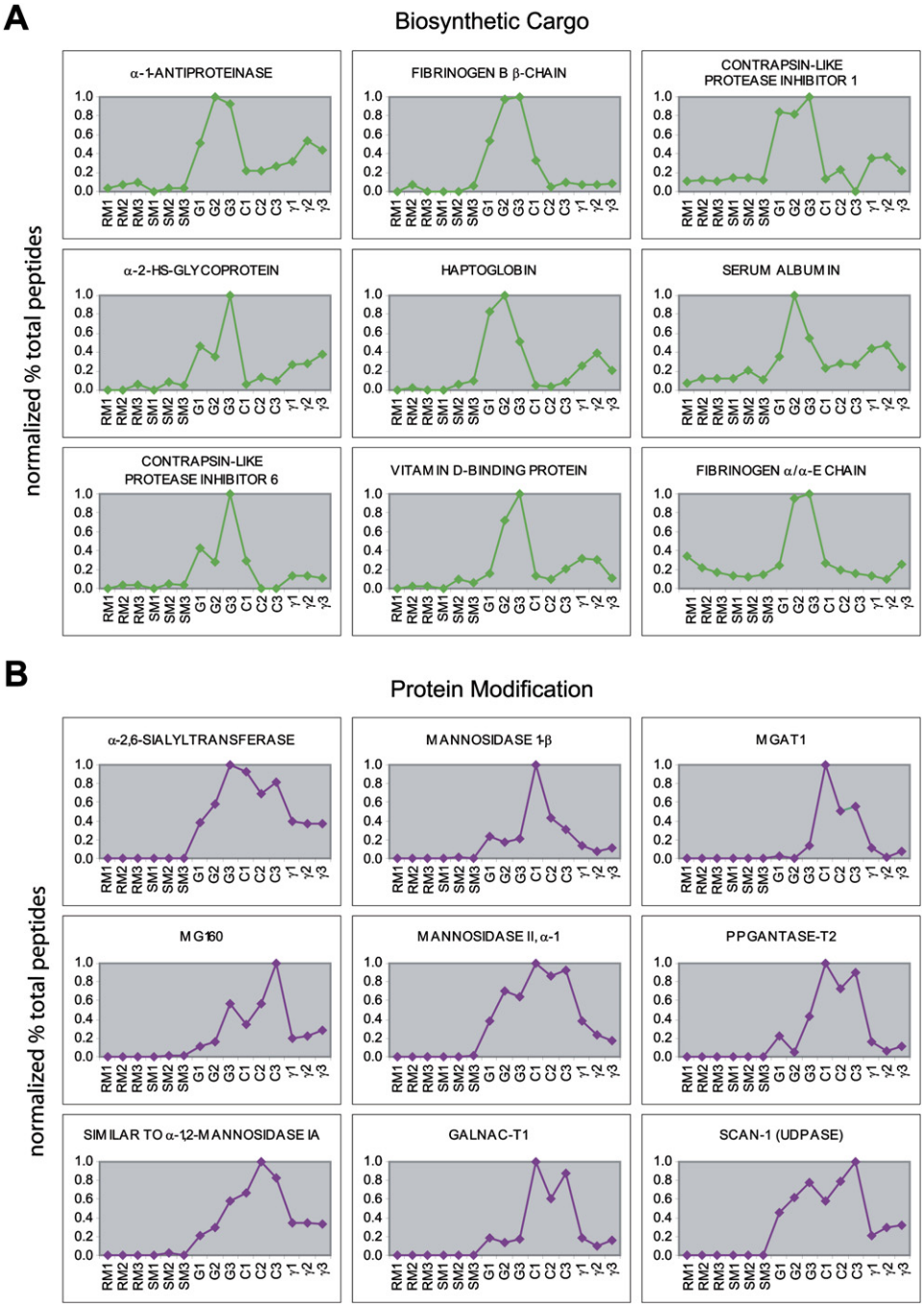

Figure 5. Cargo of COPI Vesicles Compared to RM, SM, and Golgi Fractions

(A) Nine abundant biosynthetic cargo proteins were plotted over three biological replicates of rough and smooth microsomes (RM and SM) and three Golgi (G), three COPI (C), and three COPI GTPγS (γ) fractions as normalized peptide counts. In all cases, proteins are greatly diminished in C versus G fractions.

(B) Nine abundant Golgi-resident proteins of the protein modification category are shown and plotted as in (A). In all cases, their concentration increases in C versus G fractions. Proteins with mean % total peptides ≥ 0.15% over all replicates of RM, SM, G, C, and γ fractions were selected for this figure. The maximal value (% total peptides) was set as 1.0, and all other % total peptides were normalized to the maximal value. PPGANTASE-T2 = UDP-N-acetyl-α-D-galactosamine polypeptide N-acetylgalactosaminyltransferase 2; MGAT1 = α-1,3-mannosyl-glycoprotein 2-β-N-acetylglucosaminyltransferase; SCAN-1 (UDPASE) = soluble calcium-activated nucleotidase.

proteins expected to move between the two compartments (e.g., p24s, ERGIC-53, etc.) (Table S5C).

Of the 1430 proteins assigned to the ER and Golgi (Figure 6A), 28% were integral membrane proteins (Table S1D) as predicted by TMHMM and SignalP as well as by literature searching or biochemical extraction into Triton X-114. Both the number and proportion of integral membrane proteins are higher than previously reported for organellar proteomics (Yates et al., 2005).

Comparison of Protein and RNA Expression Profiling of the Membrome (Rab GTPase Trafficking Networks)

Using mRNA expression profiles, Gurkan et al. (2005) organized membrane trafficking components into transport networks that they proposed to be coordinated by Rab-regulated protein hubs. These "membrome" networks (terminology of Gurkan et al.) should be expressed in the ER, Golgi, and COPI vesicle fractions generated in this study (we omitted the γ fraction for reasons listed above). A total of 32 Rabs were uncovered in our proteomics study (Table S1D). Twenty were identified in the total fractions of RM, SM, Golgi, and COPI vesicles (Figure 6B). Of these, Rab1A, 1B, 7, 2A, 6, 14, 10, and 18 were the most prominent. Dejgaard et al. (J.F. Presley, personal communication) have localized these Rabs by GFP tagging. Rab1A, 1B, 2A, 6, and 14 were all either exclusively Golgi localized (Rab6) or were additionally localized in the ER (Rab1A, 1B, and 2A) or endosomes (Rab14). Rab10 was detected in the ER only. Rab7 is endosomal (Chavrier et al., 1990), and its characterization here along with Rab5 may be indicative of endosomal contamination. All 32 Rabs (Table S1D) showed expression in the liver RNA profiling studies of Gurkan et al. (2005). Similarly, we found 16 SNAREs by proteomics (Figure 6B; Table S1D), 3 of which were not present in RNA expression data.

We have compared the proteins of the Rabome including Rab regulators, effectors, and related phosphatases and kinases (Figure S8A). COPI vesicle fractions show high enrichment of Rab regulators; the most prominent Rab, Rab6, is most enriched in Golgi fractions, while Rab14 appears more enriched in COPI vesicle fractions. Rab1A, 1B, and 2A appear to be distributed between Golgi and COPI vesicle fractions.

As expected, the SNAREome (Figure S8B) reveals a high abundance of Gos-28 and a sec22 homolog, as well as sec22 itself, in COPI vesicle fractions, with a variable amount in Golgi fractions. For coatomer (Figure S8C), most subunits were readily identified in the COPI vesicle fraction and a variable amount in the Golgi fractions, with the ARF guanine nucleotide exchange factor GBF-1 more restricted to the Golgi fractions. The membrome (Figure 6C) compares 90 of the genes identified by Gurkan et al. (2005) with our protein expression and localization attempts via peptide counting. Although the proteomics localization data clearly require more detailed analysis, the ease of comparing these data with transcriptional profiling is evident.

Proteins of Unknown Function

345 proteins were characterized as proteins of unknown function. As illustrated in Figure 7A, 234 were characterized in RM, SM, Golgi, and COPI vesicle fractions. Their locations are indicated by their codistribution with marker proteins. The remaining 111 proteins of unknown function were mainly of lower abundance and were found in biochemical extracts of RM, SM, and Golgi fractions or in COPI vesicle fractions generated with GTPγS (Table S1D). We validated the localization of two of the proteins in Figure 7A, as well as a protein not yet identified in rat protein databases (Figures 7B and 7C). These proteins' distributions by redundant peptide counting predict a location in the endoplasmic reticulum (Figure 7C). Using monomeric YFP, they were expressed as fusion proteins as indicated in Supplemental Experimental Procedures and revealed an ER localization (Figure 7B). During the course of our studies, one of these proteins was uncovered and localized to the cytosol (Bornhauser et al., 2003). Therefore, we raised a peptide-specific antibody to this protein, which revealed only one band by western blotting (Figure S9A). Immunolocalization confirmed the prediction for the YFP chimera—i.e., that the protein was in fact ER localized (Figure S9B). The saposin domain, the ER retrieval signal, and the cleaved signal sequence indicate that it is unlikely to be primarily cytosolic as previously reported. Localization motifs were not always found on several of the other proteins uncovered here. The elucidation of the mechanistic function of the 345 proteins may represent the discovery of a major aspect of the organellar proteomics effort and opens up new avenues of investigation for the field.

DISCUSSION

This proteomics study has provided a near complete accounting of proteins in the endoplasmic reticulum and Golgi apparatus of rat liver parenchyma. The methodology is likely applicable to all current tandem mass spectrometry-based proteomics efforts. Furthermore, the data serve as a foundation for the resolution of long-standing problems regarding the secretory pathway.

Methodology

There is a growing acceptance that the accounting of all reliably assigned (>95% probability) tandem mass spectra is related to protein abundance, and this conclusion was supported here. Isolated organelles are, however, always potentially contaminated with other compartments of the cell. Mitochondrial, peroxisomal, lysosomal, and nuclear proteins and proteins from other cells were readily detected and quantitatively accounted for by the redundant peptide counting method. We conclude that the ER fractions were contaminated with approximately 20% of proteins from other organelles but not to any appreciable extent with Golgi. The Golgi fractions were contaminated to an extent of 15% from other organelles and potentially as high as 20% from the ER.

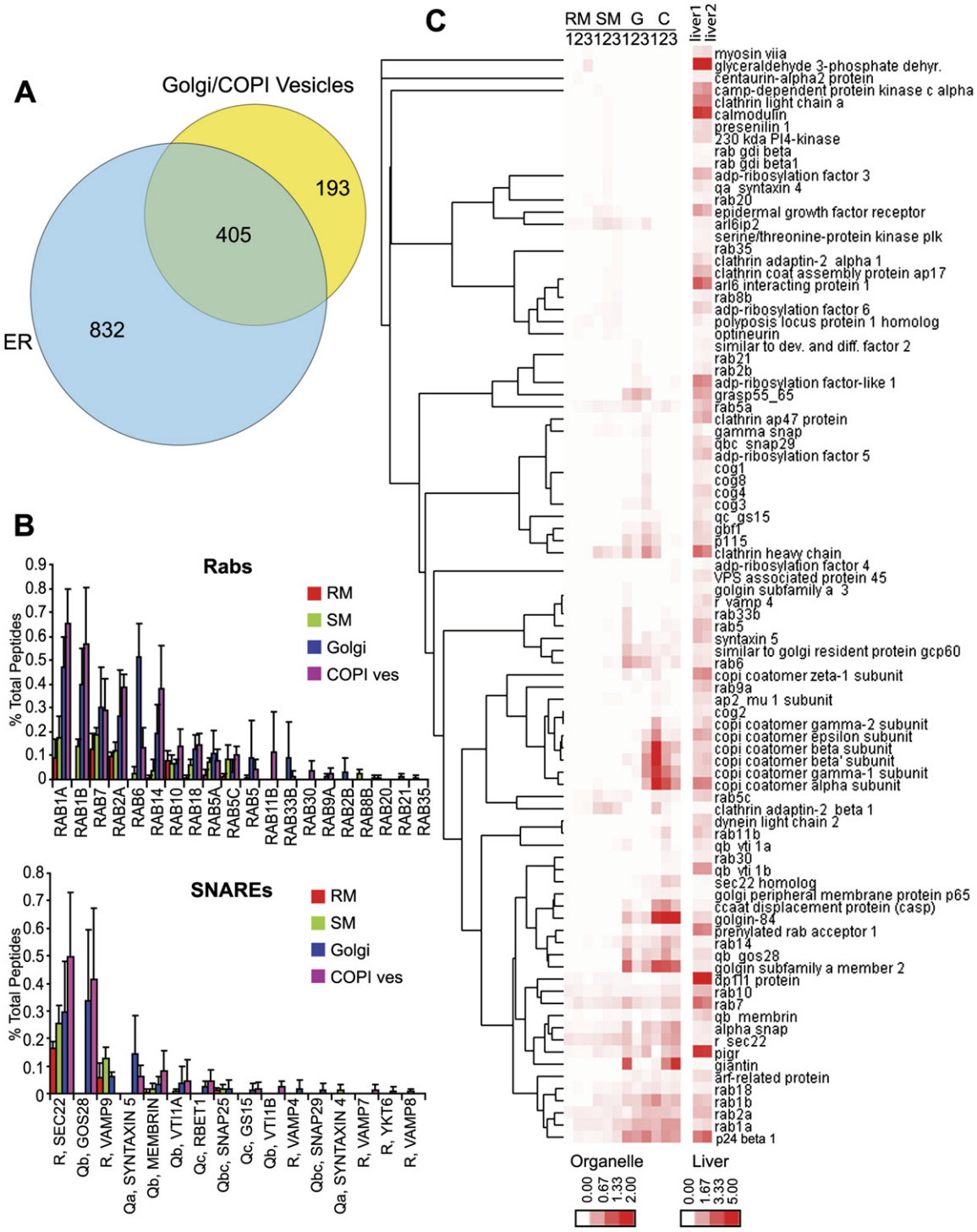

Figure 6. Proteome, Rabs, SNAREs, and Membrome of ER and Golgi Proteins of Rat Liver Parenchyma

(A) All contaminants have been removed, as well as proteins characterized as biosynthetic cargo. Proteins were considered as ER or Golgi/COPI vesicles if peptides were uniquely assigned to these proteins in RM and SM fractions (832 proteins) or Golgi/COPI vesicle fractions (193 proteins) or were shared between the two (405).

(B) Rabs and SNAREs characterized by proteomics. The mean redundant peptides assigned to Rabs and SNAREs from each subcellular fraction from Table S1D are plotted.

(C) Comparison of protein expression profiles and RNA expression profiles (liver1 and liver2) for the membrome. For (B) and (C), protein expression data are from Table S1D and liver RNA expression data are from Gurkan et al. (2005). Hierarchical clustering was applied only to the proteins, and the

By focusing on the contamination problem, ERp44 was deduced to have a predicted Golgi location by proteomics. This would be unprecedented for a PDI ortholog with a C-terminal RDEL retrieval motif. ERp44 was identified by Anelli et al. (2002) as an ER-located binding partner for Ero1 and the protein responsible for thiol-mediated retention of client proteins. The proteomics prediction was confirmed by immunolocalization with an ERp44 antibody. A predominant juxtanuclear staining pattern typical of the Golgi apparatus was observed along with a weaker perinuclear and associated reticular staining typical of the ER.

Golgi Proteome

A more global aspect of the study reported here is the extension of the Golgi proteome to COPI vesicles. The origin, existence, and biological significance of these vesicles is highly controversial (Rabouille and Klumperman, 2005). By examining a morphologically homogenous preparation that is reproducibly isolated (Figure 4), we find a consistent pattern (Figure 5A) of enrichment in Golgi-resident proteins and the near exclusion of secretory cargo. A key prediction of the cisternal maturation model is that secretory cargo remains within Golgi cisternae while Golgi-resident proteins are sorted into COPI vesicles (Malhotra and Mayor, 2006). Methodological differences in sample preparation are likely behind the apparent homogeneity of our COPI vesicle preparation (we allow for GTP hydrolysis by not excluding ARF-GAPs in our system) as compared to that of Malsam et al. (2005) (see also Rabouille and Klumperman, 2005). Therefore, these proteomics data for rat liver complement innovative imaging methods in budding yeast that have also concluded that cisternal maturation is the most likely concept to define secretory cargo delivery and test previously unresolved predictions reviewed in Malhotra and Mayor (2006). Nevertheless, as some biosynthetic transmembrane proteins were found in the vesicle fraction, the question of whether COPI vesicles transport anterograde cargo as suggested by Malsam et al. (2005) remains to be resolved.

Rabs and SNAREs

The hypothesis underlying the membrome concept of Gurkan et al. (2005) is that, given the greater diversity of Rab proteins than SNARE proteins, Rab proteins mediate the specificity required for cellular fusion events. The most prominent Rabs characterized here were Rab1A and 1B. Despite a high degree of sequence identity (>90%), the proteomics method clearly distinguished between the two. Both Rabs showed an identical distribution and relative abundance. Both have been clearly shown to regulate Golgi structure and membrane traffic through the Golgi (Alvarez et al., 2003; Wilson et al., 1994) and, as shown here, access and are concentrated in COPI vesicles. Although less well understood mechanistically, Rab2a and Rab14 are both Golgi-localized Rabs (Junutula et al., 2004; Short et al., 2001) also shown here to access COPI vesicles. These four major Rabs detected by proteomics (Figure 6B) contrast with Rab6, which, although highly concentrated in the Golgi, does not access COPI vesicles appreciably (Girod et al., 1999). Rab7 is an endosomal Rab (Chavrier et al., 1990), but it was identified here in Golgi and COPI vesicles at a concentration equal to or higher than in RM and SM fractions. Until proven otherwise, endosomal contamination is the likely explanation, even though few endosomal markers were uncovered in our proteomics study. Although 14 other Rabs were uncovered here, their abundance is demonstrably lower.

The 16 SNAREs observed here considerably extend our past proteomics effort to uncover Golgi SNAREs (Bell et al., 2001). Here, the R-SNARE sec22 and the Q-SNARE Gos-28 were the most prominent, with both accessing COPI vesicles along with the less abundant Q-SNAREs membrin, Vti-1A, B, Bet1, and GS15. By contrast, syntaxin 5 was diminished in COPI vesicles. These predicted distributions now enable more direct testing to gain mechanistic insight into SNARE-mediated fusion events in Golgi traffic.

Proteins of Unknown Function

345 proteins of unknown function were uncovered in all fractions analyzed here. A location for 234 proteins is indicated in Figure 7A, with several being unique to COPI vesicles. The elucidation of their mechanistic function linked to their location will open up an entirely new area of investigation relevant to organelle identity and trafficking mechanisms. The protein distribution predicted by proteomics was tested by chimeric YFP protein expression for three of these. During the course of our study, one of them (gi number 9903607) was described by another group as a cytosolic protein (Bornhauser et al., 2003). By contrast, we conclude an ER location by redundant peptide counting and the localization of a YFP chimera. The reticulated pattern of its localization and its saposin B domain lead to our proposal that the protein be named sapreticulin. The proteomics characterization of 345 proteins of unknown function complements the 20 new gene products uncovered in a recent RNAi screen in *Drosophila* S2 cells to identify new proteins required for Golgi function (Bard et al., 2006). Using a criterion of >50% sequence identity over the length of the protein, we identified two of these, TANGO5 (vacuole membrane protein 1, gi number 38197344) and TANGO13 (tyrosylprotein sulfotransferase 1, gi number 76779364), with identical locations (TANGO5, ER; TANGO13, Golgi) deduced from our proteomics localization method.

Completeness of the Proteome

We conclude that 1430 different proteins have been assigned to the secretory pathway (Figure 6A), although we remain uncertain about plasma membrane and endosomal contamination. An upper limit of 1424 proteins from current

RNA expression was ordered according to this clustering. RNA expression values were normalized to 100% by dividing each value by the sum of all expression values and multiplying by 100.

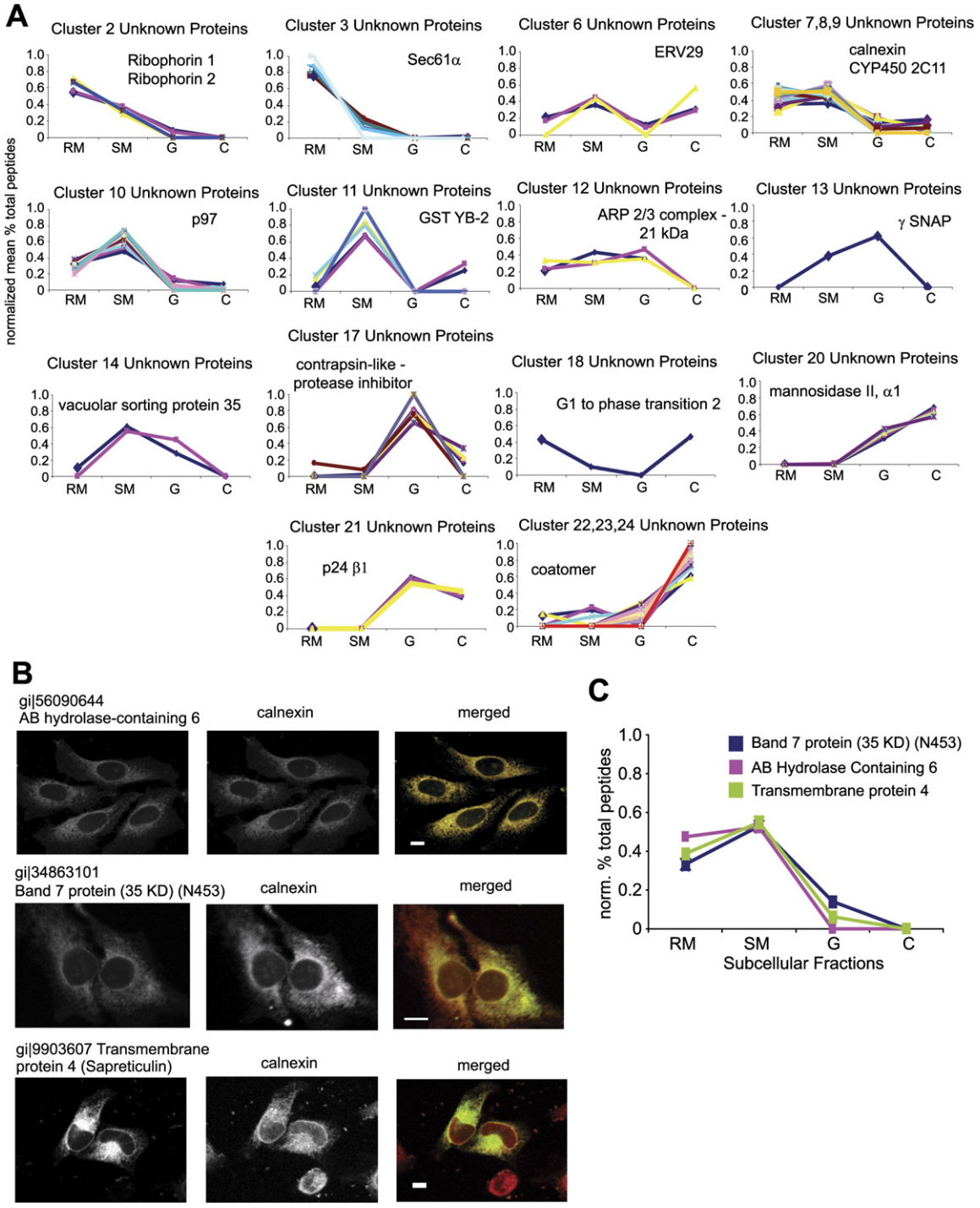

Figure 7. Distribution of Previously Uncharacterized Proteins

(A) Selection of 14 clusters with a correlation coefficient > 0.9 showing the distribution of 234 abundant proteins of unknown function, with marker proteins of each cluster indicated. The heat map used for hierarchical clustering is shown in Figure S8, and the list of proteins in each cluster is indicated in Table S3D.

(B) Verification of the localization of three selected proteins. Monomeric EYFP (mEYFP)-tagged previously uncharacterized ER proteins were transiently expressed in HeLa cells. At 24 hr after transfection, cells were fixed and permeabilized with methanol at −20°C and immunostained with anti-calnexin. Scale bars = 10 μm.

(C) Distribution of normalized peptides for the three selected proteins in the rough and smooth microsomal fractions (RM and SM) and Golgi (G) and COPI vesicle fractions (C).

bioinformatics tools is predicted from the human database for the endoplasmic reticulum (Scott et al., 2004b). Of these, 638 corresponded to proteins in our data set as deduced by BLAST. However, for those proteins that do not match our data set (Table S6), this may be due to the large number of mitochondrial or plasma membrane proteins or proteins specific to cell types other than liver parenchyma observed in this human noncurated database.

These data resolve uncertainties that arise from recent work on mouse organellar proteins (Foster et al., 2006; Kislinger et al., 2006). Kislinger et al. (2006) used a chemiluminescent western blot approach to conclude that crude fractions of liver homogenates prepared by differential centrifugation were not crosscontaminated. However, of the 567 proteins indicated with high confidence to be localized to liver microsomes, several were plasma membrane, peroxisomal, nuclear, mitochondrial, and lysosomal proteins, all of which we would consider contaminants. Indeed, as expected for such crude fractions, very few Golgi proteins were detected.

Foster et al. (2006) applied a protein correlation profiling strategy to map proteins. Here, ion intensity was used to quantify peptide and protein abundance to ten compartments of mouse liver homogenates resolved by rate zonal centrifugation. Since the Golgi represents one of these compartments, it was compared to our data set (Table S7). Of the 67 proteins concluded to be Golgi by Foster et al. (2006), our assessment indicated that only 19 were Golgi (of which 3 were COPI coatomer subunits). Thirty-five were non-Golgi and 6 were biosynthetic cargo, as indicated in Table S7. The non-Golgi proteins included nuclear (histone H2), ribosomal, and endoplasmic reticulum proteins (torsin A), all of which have been established as exclusively nuclear (histone H2) or ER (torsin A) (Hewett et al., 2003). Even highly abundant secretory proteins were poorly represented.

Therefore, highly enriched samples and an assessment of contamination by peptide counting may be a preferred strategy for organellar proteomics. The use of peptide counting to assign proteins to subcellular locations is both convenient and informative. In the current study, this strategy has led to a proteome of the hepatic ER and Golgi that may be near complete as deduced from bioinformatics predictions (Scott et al., 2004b). Furthermore, the definition of the cargo of COPI vesicles supports a role for these in cisternal maturation. Additionally, the subproteome of 345 proteins of unknown function now assigned to the secretory pathway with an organellar localization indicated by quantitative proteomics (validated for three) opens a new area of investigation wherein the combining of our proteomics database with other databases (Bard et al., 2006) can be used to mine relationships at the systems level.

EXPERIMENTAL PROCEDURES

The methodologies for organelle isolation are based on our previously published protocols (Bell et al., 2001; Dominguez et al., 1999; Kartberg et al., 2005; Paiement et al., 2005). The cell map strategy of 1D SDS-PAGE, band cutting, tandem mass spectrometry, matching of tandem mass spectra, and data analysis has been described in part previously (Bell et al., 2001; Blondeau et al., 2004; Girard et al., 2005). For more detailed aspects of these protocols and the modifications used here, see the Supplemental Experimental Procedures.

Supplemental Data

Supplemental Data include Supplemental Experimental Procedures, Supplemental References, eight tables, and ten figures and can be found with this article online at http://www.cell.com/cgi/content/full/127/6/1265/DC1/.

ACKNOWLEDGMENTS

We thank the McGill University EM facility; P.E. Scherer (Albert Einstein College of Medicine) for the antibody to ERp44; A. Fazel, S. Dejgaard, F. Blondeau, F. Laporte, D. Boismenu, F. Morales, F. Servant, S. de Grandpre, M. Drapeau, and C. Beaudrie for their help in sample preparation and data analysis; W. Balch (Scripps Research Institute) for the membrome data; M. Michalak for the luminal ER data; and I. Wada (Fukushima Medical University School of Medicine) for the generous gift of pmEYFP-N1. Financial support from the Canadian Institutes of Health Research, Genome Quebec, Genome Canada, CFI, and Valorisation-Recherche Québec is gratefully acknowledged. This study contributes to the Human Liver Proteome Project (http://www.hlpp.org/) of the Human Proteome Organization (HUPO). J.J.M.B. is a founder of Caprion Pharmaceuticals and current chair of its scientific advisory board.

Received: June 8, 2006
Revised: September 20, 2006
Accepted: October 4, 2006
Published: December 14, 2006

REFERENCES

Alvarez, C., Garcia-Mata, R., Brandon, E., and Sztul, E. (2003). COPI recruitment is modulated by a Rab1b-dependent mechanism. Mol. Biol. Cell *14*, 2116–2127.

Anelli, T., Alessio, M., Mezghrani, A., Simmen, T., Talamo, F., Bachi, A., and Sitia, R. (2002). ERp44, a novel endoplasmic reticulum folding assistant of the thioredoxin family. EMBO J. *21*, 835–844.

Bard, F., Casano, L., Mallabiabarrena, A., Wallace, E., Saito, K., Kitayama, H., Guizzunti, G., Hu, Y., Wendler, F., Dasgupta, R., et al. (2006). Functional genomics reveals genes involved in protein secretion and Golgi organization. Nature *439*, 604–607.

Bell, A.W., Ward, M.A., Blackstock, W.P., Freeman, H.N., Choudhary, J.S., Lewis, A.P., Chotai, D., Fazel, A., Gushue, J.N., Paiement, J., et al. (2001). Proteomics characterization of abundant Golgi membrane proteins. J. Biol. Chem. *276*, 5152–5165.

Benetti, R., Del Sal, G., Monte, M., Paroni, G., Brancolini, C., and Schneider, C. (2001). The death substrate Gas2 binds m-calpain and increases susceptibility to p53-dependent apoptosis. EMBO J. *20*, 2702–2714.

Blondeau, F., Ritter, B., Allaire, P.D., Wasiak, S., Girard, M., Hussain, N.K., Angers, A., Legendre-Guillemin, V., Roy, L., Boismenu, D., et al. (2004). Tandem MS analysis of brain clathrin-coated vesicles reveals their critical involvement in synaptic vesicle recycling. Proc. Natl. Acad. Sci. USA *101*, 3833–3838.

Bordier, C. (1981). Phase separation of integral membrane proteins in Triton X-114 solution. J. Biol. Chem. *256*, 1604–1607.

Bornhauser, B.C., Olsson, P.A., and Lindholm, D. (2003). MSAP is a novel MIR-interacting protein that enhances neurite outgrowth

and increases myosin regulatory light chain. J. Biol. Chem. *278*, 35412–35420.

Chavrier, P., Parton, R.G., Hauri, H.P., Simons, K., and Zerial, M. (1990). Localization of low molecular weight GTP binding proteins to exocytic and endocytic compartments. Cell *62*, 317–329.

Cox, B., Kislinger, T., and Emili, A. (2005). Integrating gene and protein expression data: pattern analysis and profile mining. Methods *35*, 303–314.

Dahan, S., Ahluwalia, J.P., Wong, L., Posner, B.I., and Bergeron, J.J. (1994). Concentration of intracellular hepatic apolipoprotein E in Golgi apparatus saccular distensions and endosomes. J. Cell Biol. *127*, 1859–1869.

Dominguez, M., Fazel, A., Dahan, S., Lovell, J., Hermo, L., Claude, A., Melancon, P., and Bergeron, J.J. (1999). Fusogenic domains of golgi membranes are sequestered into specialized regions of the stack that can be released by mechanical fragmentation. J. Cell Biol. *145*, 673–688.

Foster, L.J., de Hoog, C.L., Zhang, Y., Zhang, Y., Xie, X., Mootha, V.K., and Mann, M. (2006). A mammalian organelle map by protein correlation profiling. Cell *125*, 187–199.

Girard, M., Allaire, P.D., McPherson, P.S., and Blondeau, F. (2005). Non-stoichiometric relationship between clathrin heavy and light chains revealed by quantitative comparative proteomics of clathrin-coated vesicles from brain and liver. Mol. Cell. Proteomics *4*, 1145–1154.

Girod, A., Storrie, B., Simpson, J.C., Johannes, L., Goud, B., Roberts, L.M., Lord, J.M., Nilsson, T., and Pepperkok, R. (1999). Evidence for a COP-I-independent transport route from the Golgi complex to the endoplasmic reticulum. Nat. Cell Biol. *1*, 423–430.

Goolsby, K.M., and Shapiro, D.J. (2003). RNAi-mediated depletion of the 15 KH domain protein, vigilin, induces death of dividing and non-dividing human cells but does not initially inhibit protein synthesis. Nucleic Acids Res. *31*, 5644–5653.

Gurkan, C., Lapp, H., Alory, C., Su, A.I., Hogenesch, J.B., and Balch, W.E. (2005). Large-scale profiling of Rab GTPase trafficking networks: the membrome. Mol. Biol. Cell *16*, 3847–3864.

Hay, J.C., Hirling, H., and Scheller, R.H. (1996). Mammalian vesicle trafficking proteins of the endoplasmic reticulum and Golgi apparatus. J. Biol. Chem. *271*, 5671–5679.

Hay, J.C., Klumperman, J., Oorschot, V., Steegmaier, M., Kuo, C.S., and Scheller, R.H. (1998). Localization, dynamics, and protein interactions reveal distinct roles for ER and Golgi SNAREs. J. Cell Biol. *141*, 1489–1502.

Hewett, J., Ziefer, P., Bergeron, D., Naismith, T., Boston, H., Slater, D., Wilbur, J., Schuback, D., Kamm, C., Smith, N., et al. (2003). TorsinA in PC12 cells: localization in the endoplasmic reticulum and response to stress. J. Neurosci. Res. *72*, 158–168.

Jermy, A.J., Willer, M., Davis, E., Wilkinson, B.M., and Stirling, C.J. (2006). The Brl domain in Sec63p is required for assembly of functional endoplasmic reticulum translocons. J. Biol. Chem. *281*, 7899–7906.

Junutula, J.R., De Maziere, A.M., Peden, A.A., Ervin, K.E., Advani, R.J., van Dijk, S.M., Klumperman, J., and Scheller, R.H. (2004). Rab14 is involved in membrane trafficking between the Golgi complex and endosomes. Mol. Biol. Cell *15*, 2218–2229.

Kartberg, F., Hiding, J., and Nilsson, T. (2005). Purification of COPI vesicles. In Cell Biology: A Laboratory Handbook, J. Celis, N. Carter, K. Simons, V. Small, T. Hunter, and D.M. Shotton, eds. (Burlington, MA, USA: Elsevier Academic Press), pp. 45–50.

Kislinger, T., Cox, B., Kannan, A., Chung, C., Hu, P., Ignatchenko, A., Scott, M.S., Gramolini, A.O., Morris, Q., Hallett, M.T., et al. (2006). Global survey of organ and organelle protein expression in mouse: combined proteomic and transcriptomic profiling. Cell *125*, 173–186.

Langbein, S., Zerilli, M., Zur Hausen, A., Staiger, W., Rensch-Boschert, K., Lukan, N., Popa, J., Ternullo, M.P., Steidler, A., Weiss, C., et al. (2006). Expression of transketolase TKTL1 predicts colon and urothelial cancer patient survival: Warburg effect reinterpreted. Br. J. Cancer *94*, 578–585.

Lanoix, J., Ouwendijk, J., Lin, C.C., Stark, A., Love, H.D., Ostermann, J., and Nilsson, T. (1999). GTP hydrolysis by arf-1 mediates sorting and concentration of Golgi resident enzymes into functional COP I vesicles. EMBO J. *18*, 4935–4948.

Le-Niculescu, H., Niesman, I., Fischer, T., DeVries, L., and Farquhar, M.G. (2005). Identification and characterization of GIV, a novel Galpha i/s-interacting protein found on COPI, endoplasmic reticulum-Golgi transport vesicles. J. Biol. Chem. *280*, 22012–22020.

Malhotra, V., and Mayor, S. (2006). Cell biology: the Golgi grows up. Nature *441*, 939–940.

Malsam, J., Satoh, A., Pelletier, L., and Warren, G. (2005). Golgin tethers define subpopulations of COPI vesicles. Science *307*, 1095–1098.

Martinez-Menarguez, J.A., Prekeris, R., Oorschot, V.M., Scheller, R., Slot, J.W., Geuze, H.J., and Klumperman, J. (2001). Peri-Golgi vesicles contain retrograde but not anterograde proteins consistent with the cisternal progression model of intra-Golgi transport. J. Cell Biol. *155*, 1213–1224.

Murray, R.Z., Wylie, F.G., Khromykh, T., Hume, D.A., and Stow, J.L. (2005). Syntaxin 6 and Vti1b form a novel SNARE complex, which is up-regulated in activated macrophages to facilitate exocytosis of tumor necrosis Factor-alpha. J. Biol. Chem. *280*, 10478–10483.

Paiement, J., Young, R., Roy, L., and Bergeron, J.J. (2005). Isolation of rough and smooth membrane domains of the endoplasmic reticulum from rat liver. In Cell Biology: A Laboratory Handbook, J. Celis, N. Carter, K. Simons, V. Small, T. Hunter, and D.M. Shotton, eds. (Burlington, MA, USA: Elsevier Academic Press), pp. 41–44.

Peng, R.W. (2005). Decoding the interactions of SM proteins with SNAREs. ScientificWorldJournal *5*, 471–477.

Rabouille, C., and Klumperman, J. (2005). Opinion: The maturing role of COPI vesicles in intra-Golgi transport. Nat. Rev. Mol. Cell Biol. *6*, 812–817.

Rout, M.P., Aitchison, J.D., Suprapto, A., Hjertaas, K., Zhao, Y., and Chait, B.T. (2000). The yeast nuclear pore complex: composition, architecture, and transport mechanism. J. Cell Biol. *148*, 635–651.

Scott, M., Lu, G., Hallett, M., and Thomas, D.Y. (2004a). The Hera database and its use in the characterization of endoplasmic reticulum proteins. Bioinformatics *20*, 937–944.

Scott, M.S., Thomas, D.Y., and Hallett, M.T. (2004b). Predicting subcellular localization via protein motif co-occurrence. Genome Res. *14*, 1957–1966.

Short, B., Preisinger, C., Korner, R., Kopajtich, R., Byron, O., and Barr, F.A. (2001). A GRASP55-rab2 effector complex linking Golgi structure to membrane traffic. J. Cell Biol. *155*, 877–883.

Stojanovic, M., Germain, M., Nguyen, M., and Shore, G.C. (2005). BAP31 and its caspase cleavage product regulate cell surface expression of tetraspanins and integrin-mediated cell survival. J. Biol. Chem. *280*, 30018–30024.

Valsdottir, R., Hashimoto, H., Ashman, K., Koda, T., Storrie, B., and Nilsson, T. (2001). Identification of rabaptin-5, rabex-5, and GM130 as putative effectors of rab33b, a regulator of retrograde traffic between the Golgi apparatus and ER. FEBS Lett. *508*, 201–209.

Voeltz, G.K., Prinz, W.A., Shibata, Y., Rist, J.M., and Rapoport, T.A. (2006). A class of membrane proteins shaping the tubular endoplasmic reticulum. Cell *124*, 573–586.

Wegmann, D., Hess, P., Baier, C., Wieland, F.T., and Reinhard, C. (2004). Novel isotypic gamma/zeta subunits reveal three coatomer complexes in mammals. Mol. Cell. Biol. *24*, 1070–1080.

Wilson, B.S., Nuoffer, C., Meinkoth, J.L., McCaffery, M., Feramisco, J.R., Balch, W.E., and Farquhar, M.G. (1994). A Rab1 mutant affecting guanine nucleotide exchange promotes disassembly of the Golgi apparatus. J. Cell Biol. *125*, 557–571.

Wu, C.C., MacCoss, M.J., Mardones, G., Finnigan, C., Mogelsvang, S., Yates, J.R., 3rd, and Howell, K.E. (2004). Organellar proteomics reveals Golgi arginine dimethylation. Mol. Biol. Cell *15*, 2907–2919.

Yates, J.R., 3rd, Gilchrist, A., Howell, K.E., and Bergeron, J.J. (2005). Proteomics of organelles and large cellular structures. Nat. Rev. Mol. Cell Biol. *6*, 702–714.